HEAT GENERATION AND SIDE MILLING STABILITY OF TITANIUM ALLOY

by

Hong-Tao LI, Gang ZHAO*, Ying-Xin JI, and Yi-Chen ZHANG
School of Mechanical and Electrical Engineering, Harbin Engineering University, Harbin, China

Original scientific paper
https://doi.org/10.2298/TSCI2006033L

In this paper, the thermal generation and milling stability of titanium alloy during machining are investigated mainly. A new definition of processing behavior is given based on the principles of minimization, entity expression and combination, and a model of side milling behavior is constructed. Through a series of side milling orthogonal experiments on Ti-6Al-4V titanium alloy, the cutting forces under different process parameters are obtained. Further, the cutting force coefficients of the model is calculated by the complete average algorithm and the peak average algorithm, and the milling stability of the system is analyzed by a stability lobe diagram. The results show that the different cutting parameters have important influences on the milling stability of titanium alloy.

Key words: *titanium alloy, heat generation, milling stability, machining parameters, dynamic model*

Introduction

Being of the good corrosion resistance, high strength and high heat resistance, titanium alloy has been widely used in aero-engine impeller and blade components. However, titanium alloy is considered to be one of the toughest materials to machine due to the poor process performance and cutting performance [1]. On one hand, because of the low thermal conductivity of titanium alloy, the excessive friction heat generated near the tool tip during the milling process is not easy to be dissipate, which affects the cutting stability [2]. On the other hand, according to the research by Arrazola *et al.* [3], the chattering would occur in the machining process of titanium alloy due to its low elasticity modulus and high hardness, which may cause poor surface and low tool life.

It has been a challenge for researchers to improve the stability and avoid self-excited chatter during the machining process of titanium alloy [4]. Telrandhe *et al.* [5] found that the machining of titanium alloys can be improved after annealing. Rotella *et al.* [6] investigated the influence of the cooling conditions on surface integrity and the product performance by analyzing the results of machining of Ti-6Al-4V alloy under the cryogenic cooling conditions and the varying cutting speeds and feed rates. Wu and Zhang [7] elaborated the prominent differences of the cutting mechanisms of titanium alloy between up-milling and down-milling. Tobias *et al.* [8] noticed that in the low-speed machining process, the process damping would occur when the tool's side milling surface rubbed against the vibration surface of the work piece. Altinta and Budak [9] presented the mechanical model of process damping in low speed

* Corresponding author, e-mail: zhaogang@hrbeu.edu.cn

machining. In addition, it was very difficult to measure the temperature and predict the cutting heat distribution in the metal cutting process because of the existence of chip obstacles and the nature of continuous contact and movement between the tool and chip [10].

Generally, the machining parameters are the key factors affecting heat generation and machining process. The choosing reasonable processing parameters are helpful to achieve the good machining effect and protect the machine tools. Aiming at the process method of side milling, a model of side milling behavior is constructed in this paper, a series of side milling orthogonal experiments are conducted on Ti-6Al-4V titanium alloy, and the cutting forces under different process parameters are obtained. The cutting force coefficients of the model are calculated by the full average algorithm and the peak average algorithm, and the effects of different cutting parameters on the stability of the system are compared and analyzed. Also, the stability boundary is calculated.

Heat generation and side milling processing

Heat generation in metal milling

In the process of machining, with the tool to overcome the influence of the shear strength of the workpiece, a large amount of heat would be generated to cause a high local thermal mechanical effect on the work piece. The heat generated in metal cutting can be estimated by calorimetric or cutting force measurement. It is supposed that almost all the energy input in this process is converted into heat. The metal cutting energy consumption is expressed as follows [11]:

$$Q = FV_c \tag{1}$$

where Q is the energy consumption, F is the cutting force, and V_c is the cutting speed.

Definition of side milling processing behavior

The processing behavior refers to the behavior of process characteristics completed under the constraints of manufacturing resources and capabilities of specific design requirements between parts from raw materials to final products. Usually, the processing behavior is defined and classified according to design requirements. The processing behavior should be easy to reorganize the process and to serve the designers. The structural outline of a part is a series of geometric features formed by processing technology essentially, which are combined in a certain order.

The processing behavior contains all the parameters of the corresponding process characteristics, such as processing method, geometry, size information, accuracy information, location information, and so on. In addition, it also includes the necessary production and processing resources information for processing behavior containing multiple process behaviors.

Table 1 describes the processing behavior parameter model of the side milling. The first three parameters 001 in the behavior ID represent milling, the next 001 represent side

Table 1. Side milling processing behavior

Header	Proces action (milling)	ID (00100100X)	Side deviation (·)
Ra (·)	Start Point (·)	End Point (·)	Boolean Operation
Direction Vector (·)	Raw Materials (·)	Material (·)	Treatment Methods
Factory (·)	Enterprise (S, M, L)	Time/Cost (·)	Process Method (·)
m_side milling (KNAM, RTP, RFP, SDIS, DP, MID, FAL, FALD, FFP1, FFD, VARI, RL, AS1, LP1, FF3, AS2, LP2)			

milling, and the last number is randomly allocated for marking processing behavior. The surface roughness is Ra, and the private domain contains some information related to the manufacturer, such as processing methods, processing time, processing costs and raw material. The *m_side milling* represents the implementation function, which is an automatic generating function of CNC program for side milling.

Based on the previous work, this paper proposes a new processing behavior theorem. As shown in fig. 1, a part can be mapped to a set of processing behavior and it can be described:

$$PT_i = \{PB_a; PB_b; PB_c; ...; PB_n\} \tag{2}$$

where PT_i is the any part and PB_n is the arbitrary processing behavior. The mapping of processing behavior includes one-to-one mapping, one-to-multiple mapping, and multiple-to-one mapping. One-to-one mapping is that an element in a set of processing behaviors corresponds to an element in the process method. For example, PB_a which is in the set of processing behavior corresponds to PM_a in the set of process method and finally maps to NC_a in the set of machining program. One-to-multiple mappings is that an element in a set of processing behaviors corresponds to multiple elements in the process method. For example, PB_a which is in the set of processing behavior can correspond to PM_a, PM_b, PM_c in the set of process method and finally map to NC_a, NC_b, NC_c in the set of machining program. Multiple-to-one mappings are that multiple elements in a set of processing behaviors correspond to one element in the process method. For example, PB_a, PB_b, PB_c which are in the set of processing behavior can correspond to PM_n in the set of process method and finally map to NC_n.

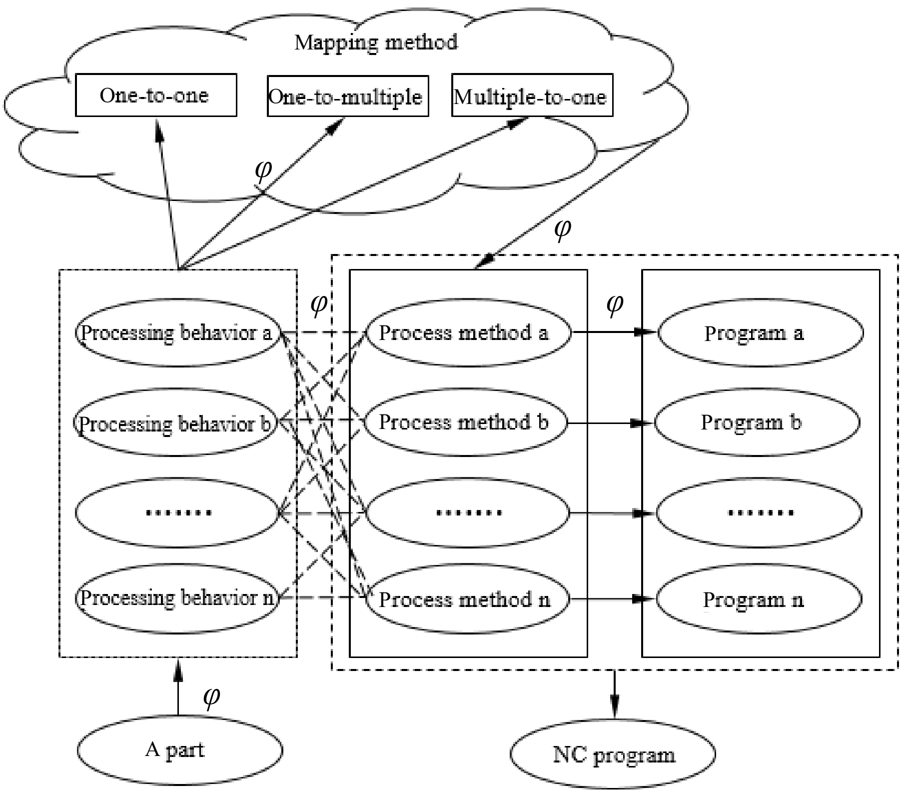

Figure 1. Mapping of the processing behavior

The part design is the combination of mapping process and process methods, and the combination of design elements is the combination of processing behavior. Processing behavior maps to process method, and then the process method maps to machining program. The combination of processing behavior and generation of numerical control program is realized by the combination mechanism of different mapping methods. The processing behavior parameters for numerical control programs can be obtained by the cutting experiments.

Constructing processing behavior knowledge database

The selections of cutting tools and cutting parameters are mostly based on the production experience. Through this kind of experience knowledge, using the production-based rule representation to express decision-making knowledge can describe the relationship between the conditions of experience knowledge and conclusions clearly. In the decision-making of cutting parameters, the cutting parameters are obtained on the basis of choosing cutting tools and taking processing conditions as input conditions. Conclusions indicate that the corresponding rules are activated by inputting conditions to obtain the tool information or the cutting parameter information meeting the conditions. Through the cutting experiments, more reliable and stable cutting parameters can be obtained, and the knowledge base of the processing behavior parameters can be constructed to realize the process automation and meet the needs of intelligent manufacturing.

Cutting force measurement experiments

Single degree-of-freedom dynamics model of milling

The single degree-of-freedom dynamics model of milling reads:

$$\ddot{x}(t)+2\zeta\omega_n\dot{x}(t)+\omega_n^2x(t)=-\frac{ah(t)}{m_t}[x(t)-x(t-T)] \tag{3}$$

where ζ denotes the damping ratio, ω_n – the natural circular frequency, a – the axial cutting depth, and m_t – the modal quality of tool. The cutting force coefficient $h(t)$ is given:

$$h(t)=\sum_{j=1}^{N}g[\phi_j(t)]\sin[\phi_j(t)]\left\{K_t\cos[\phi_j(t)]+K_r\sin[\phi_j(t)]\right\} \tag{4}$$

where K_t and K_r denote the tangential and radial cutting force coefficients, respectively, and $\phi_j(t)$ is:

$$\phi_j(t)=\frac{2\pi S}{60}t+(j-1)\frac{2\pi}{N} \tag{5}$$

The function $g[\phi_j(t)]$ is defined:

$$g[\phi_j(t)]=\begin{cases}1 & \text{if } \phi_{st}<\phi_j(t)<\phi_{ex}\\ 0 & \text{otherwise}\end{cases} \tag{6}$$

where ϕ_{st} denotes the cut-in angle, ϕ_{ex} – the cut-out angle. For the climb milling, we have that $\phi_{st}=\arccos(2a_e/D-1)$, and for the conventional milling, we have that $\phi_{ex}=\arccos(1-2a_e/D)$, where a_e/D is the ratio of radial cutting depth to tool diameter.

When $y(t)=m_t\ddot{x}(t)+m_t\zeta\omega_n(t)$ and $x(t)=[x(t)\ \ y(t)]^T$, the dynamic equation in the form of state space is expressed:

$$\dot{x}(t) = A_0 x(t) + A(t)x(t) + B(t)x(t-T) \tag{7}$$

Milling stability analysis of mode coupling effect

Considering the modal coupling effect of tool structure in milling process, the responses of *Y*-direction excitation in *X*-direction and *X*-direction excitation in *Y*-direction should not to be ignored when the modeling tool is built by the modal test method. In this way, the non-diagonal terms of the modal mass matrix, M, the damping matrix, C, and the stiffness matrix, K, are all non-zero.

In this paper, the modal parameters are obtained by modal test using the 3560C module, the acceleration sensor and the impact hammer 8206 made in Danish B&K Company. The obtained modal parameters of tool are summarized in tab. 2.

Table 2. Modal parameters of tool

M [kg]	C [Nsm^{-1}]	K [Nm^{-1}]
$\begin{bmatrix} 0.00721 & 0.0345 \\ 0.0656 & 0.00443 \end{bmatrix}$	$\begin{bmatrix} 2.310 & 3.670 \\ 9.371 & 2.834 \end{bmatrix}$	$\begin{bmatrix} 5.678\times10^5 & 1.399\times10^6 \\ 3.034\times10^6 & 3.207\times10^5 \end{bmatrix}$

Experimental scheme and parameters

In order to conduct the force measurements, the Kistler-9257B dynamometer with Kistler 5070A multi-channel amplifier was used. The experimental data were collected by the Kistler data acquisition card. The cutting tool adopted the whole carbide four-edge milling cutter. The specific parameters are shown in tab. 3.

Table 3. Tool parameters

Diameter [mm]	Teeth	Helix [°C]	Length [mm]	Material
10	4	45	70	Carbide

The four factors and four levels orthogonal test method was used to measure the cutting force of Ti-6Al-4V. The experimental data are shown in tab. 4. Figure 2 shows the variations of cutting force with time.

Table 4. Parameters applied in the four factors and four levels orthogonal test

Item	Parameters
Axial depth [mm]	0.6/ 0.8/ 1/ 1.2
Radial width [mm]	0.5/ 1/ 2/ 4
Cutting speed [mmin^{-1}]	60/ 80/ 100/ 120
Spindle speed [rpm]	2400/ 3100/ 4000/ 4800
Feed per tooth [mm]	0.04/ 0.06/ 0.10/ 0.12

Calculating the cutting force coefficients

In order to obtain the cutting force coefficients, the average cutting force is calculated firstly. Two algorithms, *i. e.* the complete averaging algorithm and peak averaging algorithm, are used to obtain the average cutting force. The complete averaging algorithm can calculate the average cutting force in several cycles and the peak averaging algorithm can calculate the average cutting force by taking the peak value of wave in several periods. Then, the cutting force coefficients can be obtained by substituting the average cutting force obtained by the above two algorithms into the cutting force formula. The calculation results of cutting force coefficients are summarized in tab. 5.

The stability lobe diagram

Considering the modal coupling effect, the stability lobe diagram obtained by the peak average cutting force method is shown in fig. 3. It is worth noting that the stability lobe diagram is calculated based on the second set of cutting force coefficients and the cut-

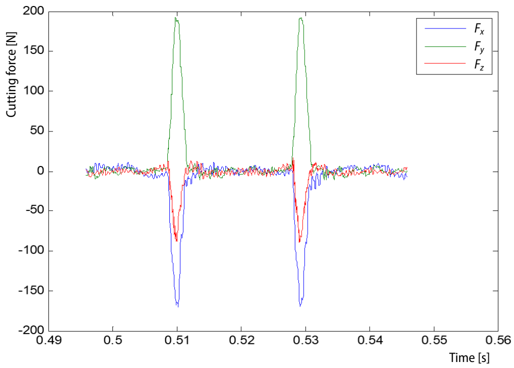

Figure 2. Changes of cutting force over time

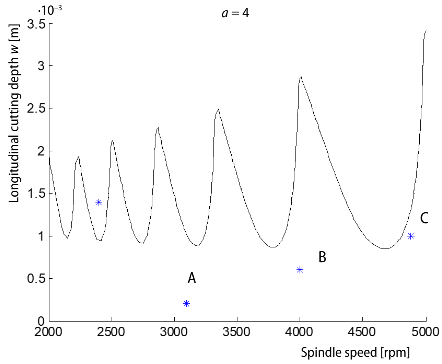

Figure 3. Stability lobe diagram at the cutting depth of 4 mm

Table 5. Calculation results of cutting force coefficients

Cutting force coefficients	Values	
	Scenario for the complete average cutting force	Scenario for the peak average cutting force
K_{tc}	2.88×10^6	-4.22×10^7
K_{te}	1.53×10^4	-1.70×10^3
K_{rc}	-6.85×10^7	4.12×10^7
K_{re}	-3.01×10^4	-0.83×10^4
K_{ac}	7.99×10^6	8.29×10^6
K_{ae}	0.92×10^4	5.71×10^4

ting depth of 4 mm. As shown in fig. 3, the wavy curve refers to the stability boundary. The unstable cutting area is above the curve, and the stable cutting area is below the curve. The stability lobe diagram of milling can reflect the influence of cutting parameters on the cutting stability. For example, the points A, B and C in stability lobe diagram reflect the influence of different cutting speeds, cutting forces and cutting heat on the cutting stability, tab. 6. Clearly, the three points are all in the stable cutting area. It indicates that the milling process is stable under these cutting parameters. Therefore, it is very important to improve the machining efficiency and quality by analyzing the stability lobe diagram under different cutting parameters.

Table 6. Summary of cutting parameters

Stable parameter points	V_c [mmin^{-1}]	F [N]	Q [W]
A	80	139.39	11151.56
B	100	109.43	10943.24
C	120	95.43	11451.14

Further, the changes of cutting force or energy consumption (cutting heat) with cutting speed are shown in fig. 4. It can be seen that the cutting force decreases with the increase of cutting speed, but the energy consumption (cutting heat) first decreases and then increases with the cutting speed. Therefore, under ensuring the cutting stability, the cutting parameters corresponding to the point B are more reasonable due to the less energy consumption.

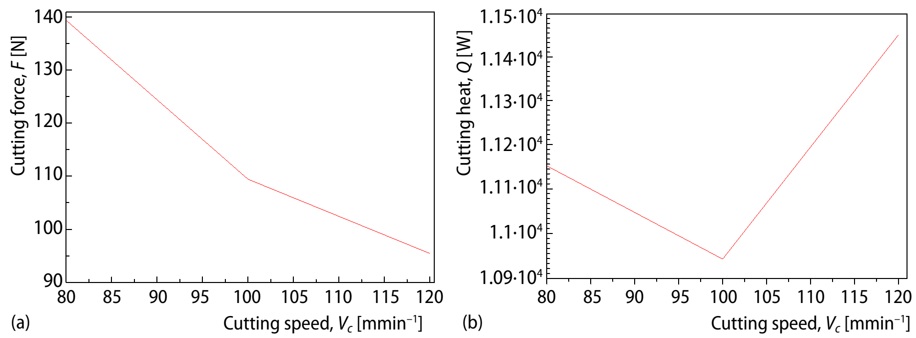

Figure 4. (a) The change of cutting force with the cutting speed and (b) the change of energy consumption with the cutting speed

Conclusion

At the present work, the new concept of the processing behavior was proposed for first time. The processing behavior resources are mapped to specific processing procedures by the mapping method and mapping template. The cutting force coefficients and the stability lobe diagram of a single degree-of-freedom dynamics model of the milling with the parameters were provided by the cutting force experiments. The different cutting parameters had the important influences on the milling stability of the titanium alloy. The obtained result provides a theoretical support for the optimization of high performance processing parameters without flutter in the milling process of the titanium alloy.

Nomenclature

a – axial cutting depth, [mm]
F – cutting force, [N]
$h(t)$ – cutting force coefficient, [–]
K_r – radial cutting force coefficient, [–]
K_t – tangential cutting force coefficient, [–]
m_t – modal quality of tool, [kg]
NC_n – machining program, [–]
PB_n – arbitrary processing behavior., [–]
PM_n – process method, [–]
PT_i – any part, [–]
Q – energy consumption, [W]
V_c – cutting speed, [mmin^{-1}]

Greek symbols

ζ – damping ratio, [–]
φ – method and mechanism of mapping
ω_n – natural circular frequency, [rads^{-1}]
ϕ_{ex} – cut-out angle, [°]
ϕ_{st} – cut-in angle, [°]

References

[1] Ezugwu, E. O., Key Improvements in the Machining of Difficult-to-Cut Aerospace Superalloys, *International Journal of Machine Tools & Manufacture*, *45* (2005), 12-13, pp. 1353-1367
[2] Ratchev, S. M., *et al.*, Mathematical Modelling and Integration of Micro-Scale Residual Stresses into Axisymmetric FE Models of Ti6Al4V Alloy in Turning, *Cirp Journal of Manufacturing ence & Technology*, *4* (2011), 1, pp. 80-89
[3] Arrazola, P. J., *et al.*, Machinability of Titanium Alloys (Ti6Al4V and Ti555.3), *J. Mater. Process. Technol.*, *209* (2009), 5, pp. 2223-2230
[4] Quintana, G., Ciurana, J., Chatter in Machining Processes: A Review, *International Journal of Machine Tools and Manufacture*, *51* (2011), 5, pp. 363-376
[5] Telrandhe, S.V., *et al.*, Effect of Microstructure and Cutting Speed on Machining Behavior of Ti6Al4V Alloy, *Journal of Mechanical Science and Technology*, *31* (2017), 5, pp. 2177-2184
[6] Rotella, G., *et al.*, The Effects of Cooling Conditions on Surface Integrity in Machining of Ti6Al4V Alloy, *International Journal of Advanced Manufacturing Technology*, *71* (2014), 1-4, pp. 47-55
[7] Wu, H., Zhang, S., Effects of Cutting Conditions on the Milling Process of Titanium Alloy Ti6Al4V, *International Journal of Advanced Manufacturing Technology*, *77* (2015), 9-12, pp. 2235-2240

[8] Tobias, S. A., Fiswick, W., *Theory of Generative Machine Tool Chatter*, The Engineer, London, UK, 1958
[9] Altinta, Y., Budak, E., Analytical Prediction of Stability Lobes in Milling, *Cirp Annals-Manufacturing Technology*, *44* (1995), 1, pp. 357-362
[10] Abukhshim, N. A., *et al.*, Heat Generation and Temperature Prediction in Metal Cutting: A Review and Implications for High Speed Machining, *International Journal of Machine Tools & Manufacture*, *46* (2006), 7-8, pp. 782-800
[11] Takeuchi, Y., *et al.*, Improvement in the Working Accuracy of an NC Lathe by Compensating for Thermal Expansion, *Precision Engineering*, *4* (1982), 1, pp. 19-24

Paper submitted: May 23, 2020
Paper revised: August 25, 2020
Paper accepted: August 30, 2020